AGU PUBLICATIONS

Geophysical Research Letters

RESEARCH LETTER
10.1002/2013GL058687

Key Points:
- Investigate the westward propagation in the North Atlantic SST observations
- Construct Climate Networks from SST data and analyze the topological properties
- Westward propagation of SST anomalies indeed seems to occur in the North Atlantic

Supporting Information:
- Readme
- SM GRL AMO fin

Correspondence to:
Q. Y. Feng,
Q.Feng@uu.nl

Citation:
Feng, Q. Y., and H. Dijkstra (2014), Are North Atlantic multidecadal SST anomalies westward propagating?, *Geophys. Res. Lett.*, *41*, doi:10.1002/2013GL058687.

Received 12 NOV 2013
Accepted 18 DEC 2013
Accepted article online 20 DEC 2013

Are North Atlantic multidecadal SST anomalies westward propagating?

Qing Yi Feng[1] and Henk Dijkstra[1]

[1]Institute for Marine and Atmospheric Research Utrecht, Department of Physics and Astronomy, Utrecht University, Utrecht, Netherlands

Abstract The westward propagation of sea surface temperature (SST) anomalies is one of the main characteristics of one of the theories of the Atlantic Multidecadal Oscillation. Here we use techniques from complex network modeling to investigate the existence of the westward propagation in the North Atlantic SST observations. We construct Climate Networks (CNs) by using a linear Pearson correlation measure (resulting in Pearson Correlation Climate Network (PCCNs)) and a (nonlinear) mutual information measure (resulting in Mutual Information Climate Network (MICNs)) of spatial correlations between SST variations. Analysis of the topological properties of both types of CNs shows that the MICNs are better in capturing the main features of propagating patterns from the noisy SST data than PCCNs and that westward propagation of multidecadal SST anomalies indeed seems to occur in the North Atlantic.

1. Introduction

The Atlantic Multidecadal Oscillation (AMO) is characterized by low-frequency variability in sea surface temperatures (SST) occurring in the North Atlantic Ocean [*Schlesinger and Ramankutty*, 1994; *Delworth and Mann*, 2000]. The AMO is thought to have significant effects on summer temperatures and precipitation variations in western Europe and North America [*Enfield et al.*, 2001; *Sutton and Hodson*, 2005] and possibly hurricane development in tropical Atlantic regions [*Andronova and Schlesinger*, 2000]. There is a debate and still unsolved question on whether the North Atlantic SST anomalies in the twentieth century is an expression of an internal climate mode or an imprint of external forcing [*Ting et al.*, 2009]. Thus, a mechanistic understanding of the AMO is important and a theory should explain the processes responsible for the multidecadal timescale and the spatial patterns of the SST anomalies [*Dijkstra et al.*, 2008].

In one of the theories of the AMO [*Te Raa and Dijkstra*, 2002], the variability arises due to internal ocean dynamics through an oscillatory instability of the background meridional overturning circulation. A sketch of this so-called thermal Rossby mode mechanism is provided in Figure 1. A warm anomaly in the north central part of the basin causes a northward meridional perturbation temperature gradient, which induces—via the thermal wind balance—an anticlockwise or westward surface zonal flow (Figure 1a). Because of a southward background temperature gradient, the anomalous anticyclonic circulation around the warm anomaly causes southward (northward) advection of cold (warm) water to the east (west) of the anomaly, resulting in westward phase propagation of the warm anomaly. Due to this westward propagation, the zonal perturbation temperature gradient becomes eastward, inducing an anticlockwise or southward surface meridional flow (Figure 1b). The resulting upwelling (downwelling) perturbations along the northern (southern) boundary cause a southward meridional perturbation temperature gradient, inducing an eastward zonal surface flow, and the second half of the oscillation starts.

In this mechanism, the basin-crossing time of the SST anomalies sets the timescale of variability and, based on the observations, it was argued to be 20–30 years [*Frankcombe et al.*, 2010]. Evidence of westward propagation was found in subsurface temperature observations [*Frankcombe et al.*, 2008], but the length of the time series (XBT data since 1960) used was relatively short. Indications for westward propagation in sea level records were found in *Frankcombe and Dijkstra* [2009] and more recently in *Vianna and Menezes* [2013], who show that after 1960, clear westward propagation in sea level occurs in the North Atlantic.

SST is certainly a complex field controlled by a diversity of (nonlinear) processes such as advection in an eddying ocean and noisy surface heat fluxes. However, it should be possible to extract westward propagating SST anomalies in the Hadley Centre Sea Ice and Sea Surface Temperature data set (HadISST), if the

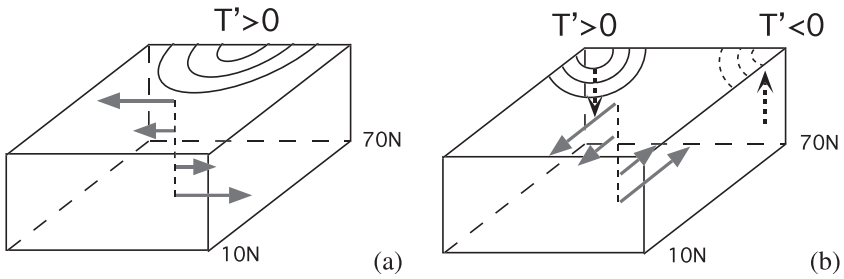

Figure 1. (a and b) Schematic diagram of the oscillation mechanism associated with the thermal Rossby mode caused by the westward propagation of the temperature anomalies T'. The phase difference between Figures 1a and 1b is about a quarter period. See text and *Te Raa and Dijkstra* [2002] for further explanation.

thermal Rossby mechanism is dominant on the multidecadal timescale (which appears to follow from sea level anomaly analysis [*Vianna and Menezes*, 2013]).

In this paper, we use new techniques based on complex network analysis [*Tsonis and Swanson*, 2006; *Gozolchiani et al.*, 2011] to investigate the existence of the westward propagation of observed North Atlantic SST anomalies. Because temporal changes in spatial correlations between climate variables do lead to temporal changes in the topological properties of the network [*Donges et al.*, 2009], this methodology provides an innovative way to study propagating patterns of climate variability.

2. Data and Methods

Since much of the AMO signal is lost when linearly detrending the SST anomaly data, for the SST observations of the North Atlantic, we use the (nondetrended) HadISST [*Rayner et al.*, 2003] data set containing monthly SST observations from January 1870 to September 2012. For more detailed information on data pretreatment, in particular the effect of detrending on the results below, we refer to section S1 of the supporting information.

To minimize the effects of the continental shape, the geographical zone we choose here is $(-51°\text{E}, -9°\text{E}) \times (9°\text{N}, 75°\text{N})$, and the resolution taken is 3°. In this way, we obtain monthly mean SST anomalies on a 14×22 spatial grid for nearly 142 years, having $N_O = 308$ nodes.

We also use data from an idealized three-dimensional single-hemispheric sector ocean model from which the mechanism of the thermal Rossby mode was originally deduced [*Te Raa and Dijkstra*, 2002]. In this model (see section S2), the ocean flow is forced only by a prescribed heat flux deduced from a steady state obtained under a fixed equator-to-pole temperature gradient. We added 10% temporally white noise to the heat flux (with a spatially coherent pattern) to excite the multidecadal variability [*Dijkstra et al.*, 2008]. The robustness of the results below the noise amplitude (up to 30% white noise) can be found in section S3. We performed a 500-year (with a time step of 0.1 year) simulation with this model. Model SST output is considered on the domain $(-66°\text{E}, -10°\text{E}) \times (10°\text{N}, 74°\text{N})$ with a 4° resolution. This provides a time series of 5000 SST anomaly fields (with respect to the time mean) on a 14×16 grid having $N_M = 224$ nodes.

For both types of data sets we constructed Climate Networks (CNs). The nodes of each CN are the locations of the grid points where we have the model data or observed data. A link between two nodes is determined by a significant interdependence between their SST anomaly time series, one of them possibly containing a lag. There are several measures of quantifying the degree of statistical interdependence, and the most common one is calculating the Pearson correlations of pairs of time series [*Tsonis and Roebber*, 2004]. We refer to such a CN as a Pearson Correlation Climate Network (PCCN). Since the Pearson correlation is a linear cross-correlation function and while in the climate system nonlinear processes possibly control the variability, we also use the mutual information (MI) based on probability distribution functions (see section S3) as a nonlinear measure of the interdependence between the time series [*Kantz and Schreiber*, 2003]. We refer to the constructed CN as a Mutual Information Climate Network (MICN). In *Donges et al.* [2009], it is shown that MI is indeed able to detect nonlinear connections between nodes more efficiently than a Pearson correlation.

Either a fixed threshold in correlation or a threshold in a fixed link density $\rho = 2E/(N(N-1))$ can be used to build unweighted and undirected links or connections among nodes in a CN; here E is the total number

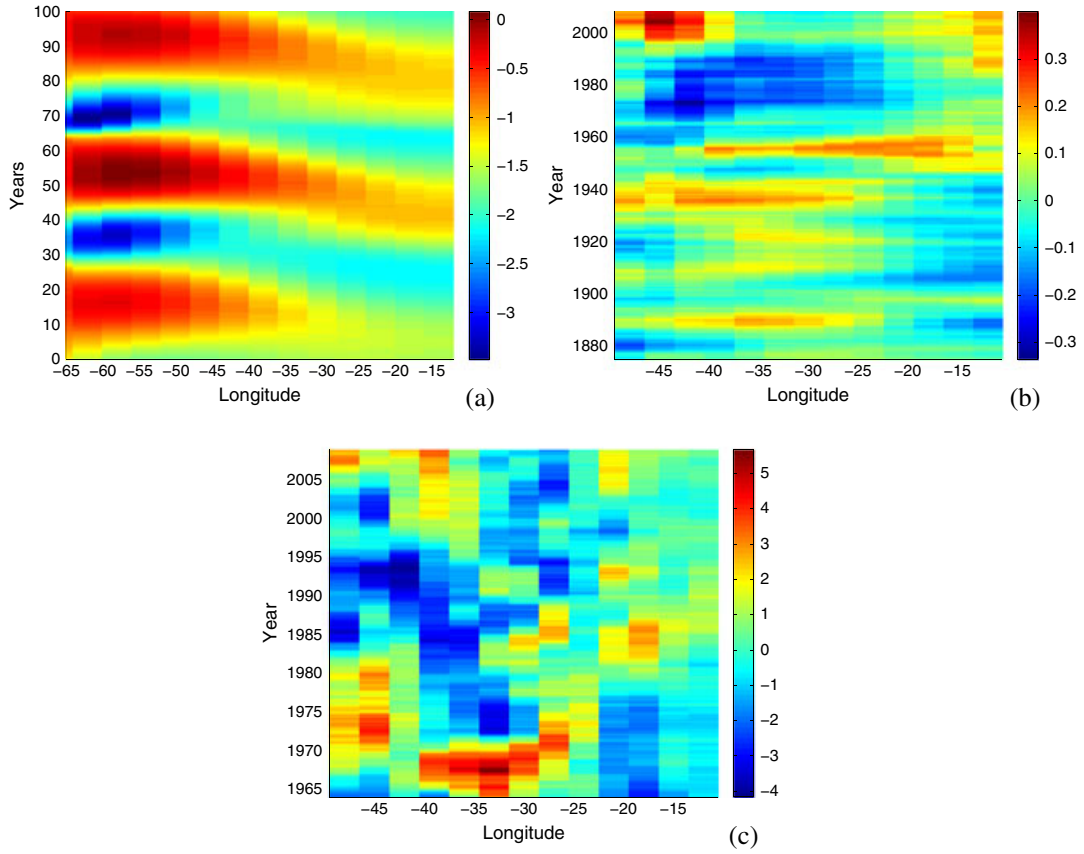

Figure 2. Hovmöller diagram of the 30–60°N averaged North Atlantic SST anomalies from (a) the idealized ocean model simulations, (b) 8-year running mean HadISST data set (1870–2012), (c) the same as Figure 2b but first the surface heat flux contribution (from the ORA-S3 data set, see http://apdrc.soest.hawaii.edu/) to SST is subtracted from HadISST data set (only over the period 1959–2009).

of links and N the total number of nodes [*Donges et al.*, 2009]. In the results below, we fix $\rho = 0.2$ which guarantees significant correlations up to the 95% level in defining the links among the nodes (see section S3 for the detailed method of CN construction) in a CN. For the topological analysis of the CNs, we only will use the degree field [*Tsonis and Swanson*, 2006; *Donges et al.*, 2009]. The degree of a node is the number of links between this node and other nodes.

3. Results

A Hovmöller diagram of meridionally averaged (30–60°N) SST anomalies from the idealized model data (Figure 2a) clearly shows the westward propagation associated with the thermal Rossby mode [*Dijkstra et al.*, 2008]. The oscillation period in the model is about 40 years, which is between the 20–30 and 50–70 dominant periods in the observations [*Frankcombe et al.*, 2010]. Note that the warm phase of the oscillation is slightly longer than the cold phase, reflecting the nonlinear effects in the variability. When a running mean of 8 years is applied to the HadISST data, a similar Hovmöller diagram (Figure 2b) does not clearly indicate westward propagation, in agreement with earlier studies [*Tourre et al.*, 1999; *Delworth and Mann*, 2000]. As part of the SST response is determined by the surface heat flux, one can do an attempt to remove this contribution (see section S1 for the method chosen). Using the surface heat flux field from the ORA-S3 reanalysis data set over the period 1959–2009 to remove this contribution from the HadISST data, the result (Figure 2c) still does not show a clear westward propagation. In addition, this correction cannot be performed over the whole HadISST data set and in addition, the correction may also remove components of the thermal Rossby wave as the surface heat flux also depends on SST.

For the Mutual Information Climate Network (MICN), the Hovmöller diagram of the relative degree field (degree divided by the maximum degree of this MICN $N_M - 1 = 223$), averaged over latitudes 30–60°N, for the idealized model data is plotted in Figure 3a. The largest lag used in the reconstruction of the MICN is

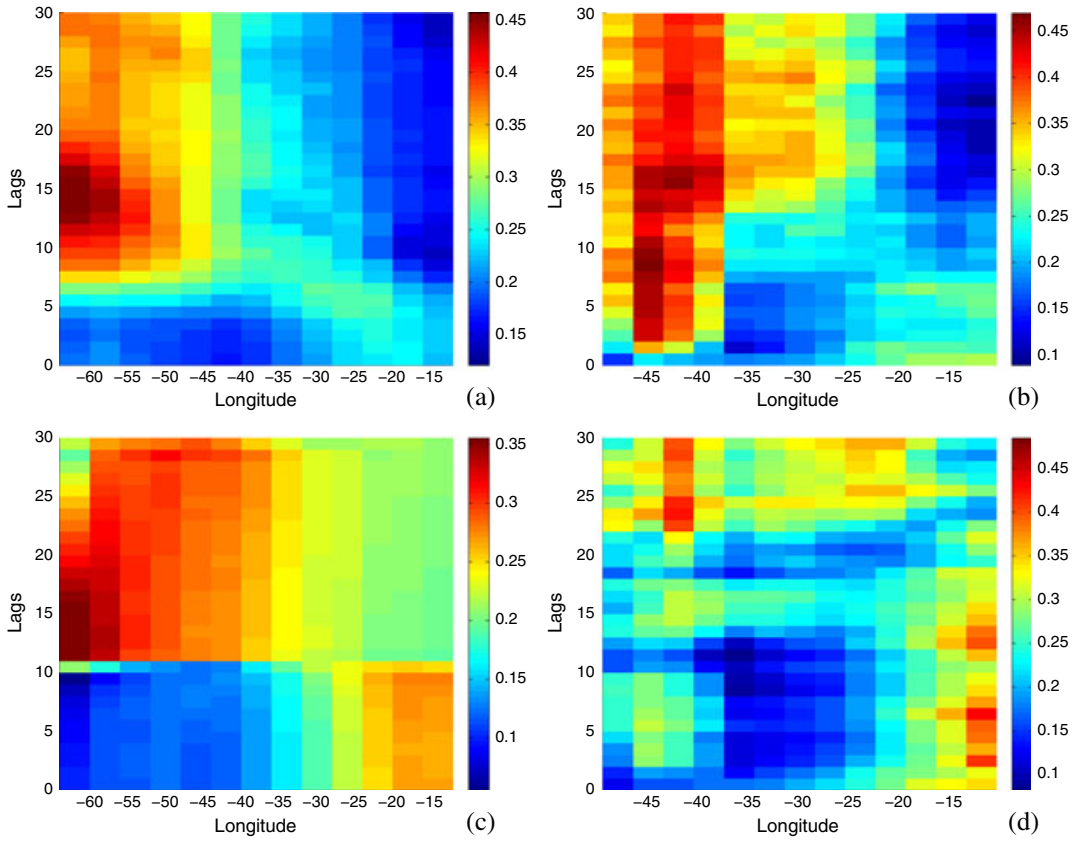

Figure 3. Hovmöller diagram of the 30–60°N averaged relative degree fields of (a and c) the idealized model data and (b and d) the observations. The networks of Figures 3a and 3b are constructed by using mutual information under a link density of 0.2. The networks of Figures 3c and 3d are constructed by using Pearson correlation under a link density of 0.2.

30 years. For small lags (0–10 years), the nodes with relatively high degree emerge from the eastern part and gradually high-degree nodes are found more westward. After approximately 15 years, the nodes with maximal degree appear at the western boundary of the domain. For the next 15 years (lags 15–30 years) there are only low-degree nodes in the eastern part, while the degrees of the nodes in the western part remain high. This is consistent with Figure 2a, where high spatial correlations are found for about 15 years in the west during the oscillation. Similar propagating features can also be found in the Hovmöller diagram of the relative degree field of the MICN constructed from the HadISST data (with $N_O - 1 = 307$), as seen in Figure 3b. There is again a westward propagation of high degree over the lags 0–10, and the maximum occurs around year 15 near −40°E. For the following 15 years, relatively high-degree nodes only appear in the western part in contrast to the lower-degree nodes in the eastern part.

A nonlinear measure of correlation, here the mutual information, appears crucial to identify the westward propagation behavior in the observations. For the Pearson Correlation Climate Network (PCCN) of the idealized model data, the Hovmöller diagram of the degree field is plotted in Figure 3c. The relative degree field (Figure 3c) shows the same features as in the MICN (compare with Figure 3a), but the position of the high-degree nodes shifts much more abruptly to the west at year 10. The relative degree field of the PCCN constructed from the observations (Figure 3d) does not show any westward propagation tendencies. In fact, the patterns of degree do not correspond neither to the one from the PCCN of the idealized model data (Figure 3c), nor to the one from the MICN of the observations (Figure 3b). Apparently, the PCCN analysis fails to distinguish the main features of the westward propagation pattern in the noisy SST signal from the observations.

To quantify the similarity between the patterns of the relative degree fields in Figures 3a and 3b, we calculate the conditional Hamming distance H_α. The Hamming distance measures the number of substitutions required to change from one string into another [*Hamming*, 1950]. We use here a conditional

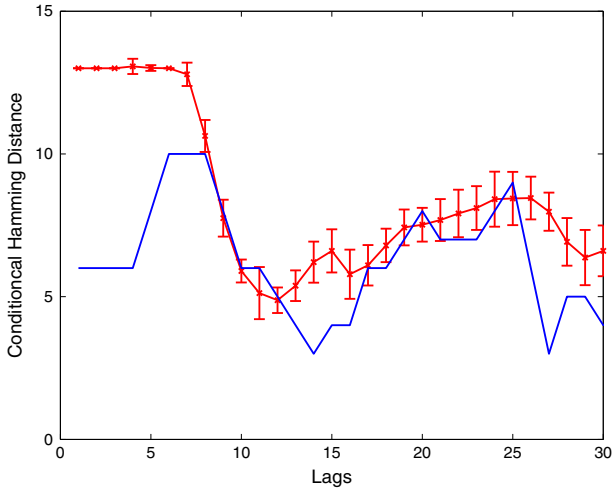

Figure 4. Conditional Hamming distance H_α (see section S4), between the relative degree field of the idealized model data and that of the observations (blue curve), for $\alpha = 0.15$. The red curve represents H_α between the relative degree field of the idealized model data and that of 200 surrogate data sets derived from the observations through shuffling; the error bars represent the standard deviation in H_α.

Hamming distance, allowing for a certain ratio of difference between two values from corresponding degree fields (represented by the fraction α); the application is detailed in section S4. The blue curve in Figure 4 is the conditional Hamming distance between the relative degree fields of the idealized model data and the observations, allowing for a 15% difference ($\alpha = 0.2$). At small lag, H_α is small but increases up to about a lag of 6 years; a second local minimum occurs around a lag of 15 years.

To evaluate the significance of this similarity measure, we use surrogate data obtained by 200 shuffled time series of the observed SST anomalies. We only randomize the sequence of the years and do not shuffle data within a particular year. Hence, the probability density function of the observed data is mostly preserved under the shuffling scheme. However, it removes the lagged correlations in the spatial pattern and hence any westward propagation (see section S4).

The red curve in Figure 4 shows the same conditional Hamming distance between the relative degree of the MICN constructed from the surrogate observations, where the error indicates the standard deviation. When the lower values of the error bars of the red curve are above the blue curve, the value of the conditional Hamming distances shows a significant similarity between the degree fields of the observations and the idealized model data and hence indicates the existence of westward propagation.

Significance is most prominent near the minima of the blue curve which are in the 10–15 year and 25–30 year timescale.

This result is robust over quite a large range of α values (see section S4).

4. Discussion

The thermal Rossby mode mechanism is a promising candidate to explain multidecadal (20–30 years) climate variability in the North Atlantic [*Frankcombe et al.*, 2010]. One of the limitations of the theory is that the spatial patterns of variability have so far only been obtained in ocean-only models [*Sevellec and Fedorov*, 2013]. One of the main characteristics of the thermal Rossby mode mechanism is the westward propagation of temperature anomalies. Indications for westward propagation were found in observed subsurface temperature fields [*Frankcombe et al.*, 2008] and sea level records [*Frankcombe and Dijkstra*, 2009; *Vianna and Menezes*, 2013]. However, this property was difficult to distinguish from SST observations because many other processes affect SST in the North Atlantic [*Sutton and Hodson*, 2005; *Booth et al.*, 2012].

We have studied the westward propagation of North Atlantic SST anomalies by analyzing the topological properties of Climate Networds (CNs) constructed using Mutual Information (MI) from idealized model data (with only the thermal Rossby mode) and from the observations. The relative degree field of the MICNs from the observations show similar propagation properties as the one of MICNs constructed from the idealized model results, and the conditional Hamming distance provides a quantitative measure of this similarity. Differences between network properties of the MICNs of the idealized model data and the observations may occur due to (i) additional processes affecting SST variability, (ii) the pretreatment of the observations, and (iii) the effect of the continental boundaries (in the observations). A limitation of the methodology used here is that it is difficult to determine where these differences originate from.

A good correspondence between observations and idealized model data cannot be clearly seen by using the (linear) Pearson Correlation (PC) to construct networks (PCCNs). The SST anomaly field is thought

to result from advective contributions as well as from a noisy surface heat flux field. In addition, the growth rate of the thermal Rossby mode is known to depend on the time-dependent background state [*Dijkstra et al.*, 2008].

This introduces nonlinear dependencies in the propagation of the mode which may be the reason that the MI is better suited to detect these features instead of the PC.

Finally, this study demonstrates that tools from complex network analysis provide an innovative way to detect spatial propagation of patterns of variability in the climate system. These tools can be directly applied to results from General Circulation Models and can also be extended to look at (lagged) spatial correlations between different fields.

Acknowledgments
The authors thank Jonathan Donges, Norbert Marwan, and Reik Donner (PIK, Potsdam) for providing the software package "pyUnicorn" used in the network calculations here. The authors would like to acknowledge the support of the LINC project (289447) funded by ECs Marie-Curie ITN program (FP7-PEOPLE-2011-ITN). Q.F. also thanks Avi Gozolchiani (Bar-Ilan University, Ramat-Gan), Alexis Tantet, and Matthijs den Toom (IMAU, Utrecht) for constructive suggestions and technical support.
The Editor thanks two anonymous reviewers for their assistance in evaluating this paper.

References

Andronova, N., and M. Schlesinger (2000), Causes of global temperature changes during the 19th and 20th centuries, *Geophys. Res. Lett.*, *27*(14), 2137–2140.
Booth, B. B., N. J. Dunstone, P. R. Halloran, T. Andrews, and N. Bellouin (2012), Aerosols implicated as a prime driver of twentieth-century North Atlantic climate variability, *Nature*, *484*(7393), 228–232.
Delworth, T., and M. Mann (2000), Observed and simulated multidecadal variability in the Northern Hemisphere, *Clim. Dyn.*, *16*(9), 661–676.
Dijkstra, H. A., L. M. Frankcombe, and A. S. Von der Heydt (2008), A stochastic dynamical systems view of the Atlantic Multidecadal Oscillation, *Philos. Trans. R. Soc. A*, *366*(1875), 2543–2558.
Donges, J. F., Y. Zou, and N. Marwan (2009), The backbone of the climate network, *Europhys. Lett.*, *87*, 48007.
Enfield, D., et al. (2001), The Atlantic Multidecadal Oscillation and its relation to rainfall and river flows in the continental U.S., *Geophys. Res. Lett.*, *28*(10), 2077–2080.
Frankcombe, L., H. Dijkstra, and A. Von der Heydt (2008), Sub-surface signatures of the Atlantic Multidecadal Oscillation, *Geophys. Res. Lett.*, *35*, L19602, doi:10.1029/2008GL034989.
Frankcombe, L. M., and H. A. Dijkstra (2009), Coherent multidecadal variability in North Atlantic sea level, *Geophys. Res. Lett.*, *36*, L15604, doi:10.1029/2009GL039455.
Frankcombe, L. M., A. S. Von Der Heydt, and H. A. Dijkstra (2010), North Atlantic multidecadal climate variability: An investigation of dominant time scales and processes, *J. Clim.*, *23*(13), 3626–3638.
Gozolchiani, A., S. Havlin, and K. Yamasaki (2011), Emergence of El Niño as an autonomous component in the Climate Network, *Phys. Rev. Lett.*, *107*(14), 148501.
Hamming, R. W. (1950), Error detecting and error correcting codes, *Bell System Tech. J.*, *26*, 147–157.
Kantz, H., and T. Schreiber (2003), *Nonlinear Time Series Analysis*, vol. 7, Cambridge Univ. Press, Cambridge, U. K.
Rayner, N., D. Parker, E. Horton, C. Folland, L. Alexander, D. Rowell, E. Kent, and A. Kaplan (2003), Global analyses of sea surface temperature, sea ice, and night marine air temperature since the late nineteenth century, *J. Geophys. Res.*, *108*(D14), 4407, doi:10.1029/2002JD002670.
Schlesinger, M., and N. Ramankutty (1994), An oscillation in the global climate system of period 65–70 years, *Nature*, *367*(6465), 723–726.
Sevellec, F., and A. V. Fedorov (2013), The leading, interdecadal eigenmode of the Atlantic Meridional Overturning Circulation in a realistic ocean model, *J. Clim.*, *26*(7), 2160–2183.
Sutton, R., and D. Hodson (2005), Atlantic Ocean forcing of North American and European summer climate, *Science*, *309*(5731), 115–118.
Te Raa, L. A., and H. A. Dijkstra (2002), Instability of the thermohaline ocean circulation on interdecadal timescales, *J. Phys. Oceanogr.*, *32*(1), 138–160.
Ting, M., Y. Kushnir, R. Seager, and C. Li (2009), Forced and internal twentieth-century SST trends in the North Atlantic, *J. Clim.*, *22*(6), 1469–1481.
Tourre, Y. M., B. Rajagopalan, and Y. Kushnir (1999), Dominant patterns of climate variability in the Atlantic Ocean during the last 136 years, *J. Clim.*, *12*, 2285–2299.
Tsonis, A. A., and P. J. Roebber (2004), The architecture of the climate network, *Physica A*, *333*, 497–504.
Tsonis, A. A., and K. L. Swanson (2006), What do networks have to do with climate? *Bull. Am. Meteorol. Soc.*, *87*(5), 585–595.
Vianna, M. L., and V. V. Menezes (2013), Bidecadal sea level modes in the North and South Atlantic Oceans, *Geophys. Res. Lett.*, *40*, 5926–5931, doi:10.1002/2013GL058162.